

Constraints on σ_8 from galaxy clustering in N -body simulations and semi-analytic models

Geraint Harker,^{1,2*} Shaun Cole¹ and Adrian Jenkins¹

¹*Department of Physics, University of Durham, Science Laboratories, South Road, Durham DH1 3LE*

²*Kapteyn Astronomical Institute, University of Groningen, PO Box 800, 9700AV Groningen, the Netherlands*

9 November 2018

ABSTRACT

We generate mock galaxy catalogues for a grid of different cosmologies, using rescaled N -body simulations in tandem with a semi-analytic model run using consistent parameters. Because we predict the galaxy bias, rather than fitting it as a nuisance parameter, we obtain an almost pure constraint on σ_8 by comparing the projected two-point correlation function we obtain to that from the SDSS. A systematic error arises because different semi-analytic modelling assumptions allow us to fit the r -band luminosity function equally well. Combining our estimate of the error from this source with the statistical error, we find $\sigma_8 = 0.97 \pm 0.06$. We obtain consistent results if we use galaxy samples with a different magnitude threshold, or if we select galaxies by b_J -band rather than r -band luminosity and compare to data from the 2dFGRS. Our estimate for σ_8 is higher than that obtained for other analyses of galaxy data alone, and we attempt to find the source of this difference. We note that in any case, galaxy clustering data provide a very stringent constraint on galaxy formation models.

Key words: cosmology: theory – dark matter – galaxies: haloes – galaxies: formation

1 INTRODUCTION

For a given set of cosmological parameters in Λ CDM, the clustering of dark matter can be studied very accurately through N -body simulations (e.g., Springel et al. 2005), or for that matter, through analytic models calibrated by simulations (e.g., Smith et al. 2003). The clustering of dark matter is not usually observed directly, however, though weak lensing shear-shear correlations can provide (at present noisy) estimates. Redshift surveys may furnish us with galaxy clustering statistics (see, e.g., Peacock 2003), while weak lensing measurements, for example, normally probe the cross-correlation between galaxies and dark matter (Refregier 2003, and references therein).

Galaxy clustering statistics derive a great deal of their power to constrain cosmological parameters by constraining the scale at which the power spectrum ‘turns over’ on large scales, which complements the high-redshift CMB constraint on this scale rather well. The baryonic features in the correlation function or power spectrum add to the effectiveness of the constraint (Cole et al. 2005; Eisenstein et al. 2005). The scales used in these joint constraints tend to be large scales, where the evolution of clustering is still in the linear regime or where deviations from linearity can be more readily modelled. Moreover, in this regime the galaxy correlation function is expected, in the absence of non-local effects, to have the same shape as the mass correlation function, though offset by a constant factor (see, e.g., Coles 1993). This offset – the (square of

the) bias – depends on the galaxy population under consideration; it depends, for example, on the threshold luminosity of the sample. Because of this uncertainty, when the galaxy correlation function is used to constrain cosmology, information on its overall normalization is not normally used, and the constraints come entirely from its shape.

In this paper we generate synthetic galaxy clustering statistics by painting galaxies from a semi-analytic model onto dark matter distributions given by N -body simulations. We then compare these clustering statistics with those from the SDSS to attempt to constrain cosmology. We can see the possibility for various benefits from our approach. Firstly, because we attempt to generate realistic catalogues with full galaxy properties, we can make a *prediction* for the bias factor of a given galaxy sample and hence use the overall normalization of the correlation function in our cosmological constraints. In particular, we may be able to constrain σ_8 , which is not possible for normal techniques employing galaxy clustering. Secondly, because we populate the simulations on a halo-by-halo basis rather than just assuming that galaxies approximately trace mass on large scales, we generate a theoretical prediction for the small-scale, nonlinear clustering. We can therefore attempt to use this information in our cosmological constraints too.

Our constraints are largely independent from those using the CMB, and involve different assumptions (though we consider only flat models, which one could regard as implicitly using CMB results). Because dark energy has an effect on structure formation, and different forms of dark energy might affect it in different ways at late times, it is useful to have an independent,

* E-mail: harker@astro.rug.nl

low-redshift constraint on σ_8 that does not rely on a joint analysis with high-redshift data (Doran, Schwindt & Wetterich 2001; Bartelmann, Doran & Wetterich 2006). A joint analysis would tend to be more model-dependent as one must be able to model what happens in the gap between observed snapshots of the Universe.

2 CONSTRUCTING GALAXY CATALOGUES

2.1 Simulations

In choosing parameters for our simulations, our aim was to generate simulation outputs for a range of different values of Ω_M and σ_8 so that we could examine galaxy clustering as a function of these quantities. Given our focus on constraining σ_8 , we opted to generate outputs with σ_8 taking values between 0.65 and 1.05, regularly spaced in steps of 0.05.

Measurements of the abundance of clusters constrain the high-mass end of the halo mass function, and hence constrain a combination of Ω_M and σ_8 (e.g., Eke, Cole & Frenk 1996). This combination is, very approximately, $\sigma_8 \Omega_M^{0.5}$. To test if we could break this degeneracy, we have generated two grids of models. For Grid 1, the parameters of each model satisfy $\sigma_8 \Omega_M^{0.5} = 0.8(0.3)^{0.5}$, while for Grid 2 they satisfy $\sigma_8 \Omega_M^{0.5} = 0.9(0.3)^{0.5}$. Within each grid, σ_8 takes on its full range of values between 0.65 and 1.05. It would be very difficult to distinguish between two cosmologies lying on the same grid using cluster abundances. The two ‘cluster normalization’ curves, with $\sigma_8 \Omega_M^{0.5} = \text{const.}$, are shown as the long-dashed and short-dashed lines in Fig. 1. The pairs (Ω_M, σ_8) labelling the cosmologies we analyse are plotted as crosses on these curves.

We extract the mass distribution for these cosmologies from two simulations run using the TREE-PM N -body code GADGET2 (Springel, Yoshida & White 2001; Springel 2005). Each simulation follows the evolution of 512^3 particles in a $300 h^{-1}$ Mpc box. We have stored the simulation output at several redshifts. Each of these snapshots of the mass distribution is then interpreted as a $z = 0.1$ snapshot of a simulation with a different cosmology, to avoid having to run a great number of simulations. We choose $z = 0.1$ since this is near the median redshift of the main SDSS and 2dFGRS galaxy samples. The output redshifts are chosen so that once the simulations are relabelled as $z = 0.1$ snapshots, the value of σ_8 at $z = 0$ for each simulation falls onto a regular grid. Each simulation then gives us snapshots with σ_8 taking values between 0.65 and 1.05, regularly spaced by 0.05. Table 1 gives the value of Ω_M and σ_8 in these relabelled snapshots. We have chosen the simulation parameters such that the first simulation, ‘Run 1’, has $\Omega_M = 0.3$ at its $\sigma_8 = 0.8$ output, while the second simulation, ‘Run 2’, has $\Omega_M = 0.3$ at its $\sigma_8 = 0.9$ output. When we perform a further rescaling of Ω_M (see below) it is these central snapshots which remain unchanged. The initial conditions are calculated using a Bardeen et al. (1986) power spectrum with shape parameter $\Gamma = 0.14$ and with primordial spectral index $n_s = 1$. A smooth power spectrum was most convenient in the light of the rescalings we carry out on the final output, but in fact the Bardeen et al. (1986) power spectrum with $\Gamma = 0.14$ was found to be a good fit to the CMBFAST (Seljak & Zaldarriaga 1996) spectrum with $\Omega_b = 0.045$ used for the Millennium Simulation (Springel et al. 2005), the parameters of which were chosen to be in agreement with the one-year WMAP results (Spergel et al. 2003).

Once we have relabelled the simulation snapshots as $z = 0.1$ snapshots, they lie on a curve in (Ω_M, σ_8) space which reflects the way the dark matter density is reduced and the amplitude of

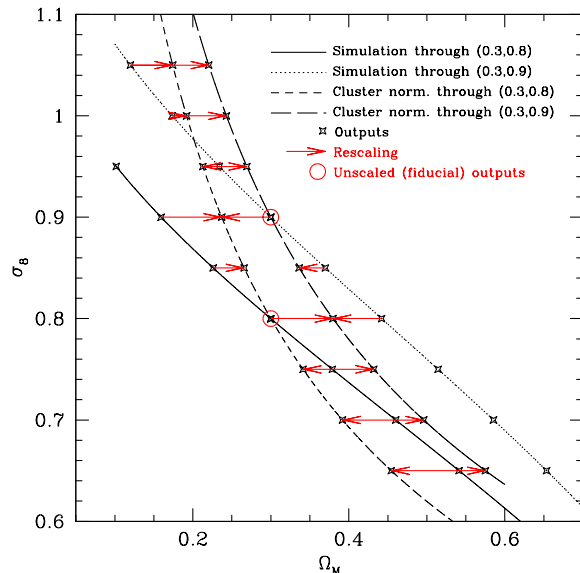


Figure 1. The position in the (Ω_M, σ_8) plane of the outputs of our two simulations. The line connecting the outputs shows how the values of Ω_M and σ_8 change as the simulation evolves, where we track the instantaneous values of these parameters rather than the values they will have at the final time, which would be the more conventional labelling (and would, of course, not change during the course of the simulation). The solid line corresponds to Run 1 and the dotted line corresponds to Run 2. Low redshift outputs (lower density, more clustered) are in the top left, while high redshift outputs (higher density, less clustered) are in the bottom right. Also shown are the curves described by the cluster normalization condition that $\sigma_8 \Omega_M^{0.5} = \text{const.}$ for two different values of this constant. We rescale simulation outputs so that they lie on these curves. The rescaling is shown schematically by the red arrows.

clustering is increased as the simulation evolves. These curves are shown as the solid and dotted lines in Fig. 1. We rescale Ω_M in each snapshot, so that instead the snapshots lie on one of the cluster-normalized curves described above. The rescaling is achieved in practice by applying the results of Zheng et al. (2002). If the particle mass is scaled in the obvious way to obtain the desired Ω_M , the particle velocities must also be scaled to compensate, else the haloes no longer satisfy the virial relation between their kinetic and potential energy, and the galaxy populations of haloes are easily distinguished in the different cosmologies via dynamical observables. The rescalings in Ω_M which move a snapshot onto the cluster-normalization curve are shown schematically as red arrows in Fig. 1. Each cluster-normalized grid contains rescaled snapshots from both simulations, and the simulation parameters were chosen so that the rescalings would never have to be too large. For some of the cosmologies on our grid, we could choose to rescale from either of our simulation runs without having to change Ω_M by a large factor. We have used these cosmologies to test that the results using either simulation run are consistent, and hence that our rescaling works as expected.

The simulation code runs SUBFIND (Springel et al. 2001) on the fly, providing us with a list of friends-of-friends haloes (Davis et al. 1985) of more than 20 particles, and their substructures. We use a linking length of 0.2 times the mean inter-particle separation in the friends-of-friends algorithm to identify the haloes. SUBFIND also allows us to identify the particle in the halo with

Table 1. Cosmological parameters of simulation outputs after having been relabelled as $z = 0.1$ outputs. We follow the usual convention that these are the parameter values the simulation would have if evolved further to $z = 0$.

Run 1		Run 2	
Ω_M	σ_8	Ω_M	σ_8
		0.120	1.050
		0.173	1.000
0.102	0.950	0.234	0.950
0.159	0.900	0.300	0.900
0.226	0.850	0.370	0.850
0.300	0.800	0.442	0.800
0.379	0.750	0.514	0.750
0.460	0.700	0.585	0.700
0.541	0.650	0.654	0.650

the least gravitational potential energy, which we use in our galaxy placement scheme.

2.2 Semi-analytic model

The properties of galaxies in our catalogues are generated using the semi-analytic galaxy formation code, GALFORM (Cole et al. 2000; Benson et al. 2002, 2003; Baugh et al. 2005). For the purposes of this paper, we may consider a semi-analytic model as being a means of predicting, given some dark matter halo at a redshift of interest, the galaxy population of that halo. Having that information, we can construct galaxy luminosity functions, correlation functions, etc. that might be considered the results or predictions of the model.

The first step in predicting the galaxy population of a halo is calculating the merger history of the halo. In simulations of sufficiently high resolution and with a sufficiently large number of outputs, this can be extracted from the N -body data. In the case of GALFORM, this has been done recently by Bower et al. (2006) with the Millennium Simulation (Springel et al. 2005); the same simulation has also been used by Croton et al. (2006) and De Lucia et al. (2006) to generate catalogues using a different semi-analytic code. The simulations we describe above, by contrast, do not have sufficient resolution for us to extract reliable merger trees for the haloes of interest. A Monte Carlo scheme based on the work of Lacey & Cole (1993) and using the algorithm described by Cole et al. (2000) is employed instead, therefore. This generates a merger tree for a halo based only on the halo mass, the cosmology and the initial power spectrum, and does not use other data from the simulation. This scheme does not, therefore, provide galaxy positions; our method of placing galaxies is given, instead, in Section 2.3.

Unfortunately, the statistical properties of merger histories generated by this algorithm are not identical to histories extracted directly from an N -body simulation (Cole et al. 2007). Parkinson, Cole & Helly (2007) and Neistein & Dekel (2007) have devised empirically motivated modifications to the algorithm to allow Monte Carlo trees to fit the simulation data better. A detailed analysis of the effect of such a modification on semi-analytic galaxy properties is beyond the scope of this paper. We have, though, tested some of our results using the new algorithm of Parkinson et al. (2007), and find that for our purposes the new trees make little difference.

Given the merger history of a halo, the model computes the evolution of the baryonic content of the halo using a variety of analytic prescriptions. Many of the equations governing the physical processes modelled by GALFORM contain parameters which may

be adjusted. Some of these (for example, the form factor f_{orbit}/c which governs the size of merger remnants) have a ‘natural’ value determined by the physics; others (those governing the angular momentum distribution of infalling haloes, say) are derived by comparison to more detailed simulations. The function of allowing these parameters to change, then, is to allow investigation into the magnitude of the effect of different physical processes on the resulting galaxy properties in the model. Other parameters have no natural value, and can only be fixed by requiring that they take values which allow the model to fit observations. Much of the time, if we are able to fit some set of observations satisfactorily by choosing the parameters of the model judiciously, the same set of observations could also be fit reasonably well by some very different choice of parameters. Therefore, within the GALFORM framework, we have different models using different physics which are equally good at matching the observations (though this may not, of course, be the case if we were to choose a different set of observations to constrain the model).

Our aim here is to try to constrain cosmological parameters by comparing clustering statistics from a simulation populated with semi-analytic galaxies to the corresponding measurements in an observational survey. We would hope that our constraints are insensitive to the precise semi-analytic model used, and we would like to test whether this is the case. Therefore, although we use only one code, GALFORM, we use three different ‘models’, in the sense of different combinations of the physics we attempt to model and the parameters governing that physics. In the remainder of this section of the paper, we discuss the technical differences between the three models before briefly describing how galaxies are placed in the simulations in Section 2.3. A reader uninterested in the details of the models may therefore wish to skip to 2.3, or to our results in Section 3. The three models are as follows:

- The fiducial model of Cole et al. (2000). This is successful in matching several sets of observations, including the B - and K -band luminosity functions, galaxy colours and mass-to-light ratios for galaxies of different morphologies, the cold gas mass in galaxies, galaxy disc sizes and the slope and scatter of the I -band Tully-Fisher relation. Unfortunately, though, it assumes a cosmic baryon fraction, Ω_b , of only 0.02. This is inconsistent with recent estimates from Big Bang nucleosynthesis (e.g., O’Meara et al. 2001) and the cosmic microwave background (Spergel et al. 2007). Nevertheless, we feel it is worthwhile to include this model in our analysis as a well recognized and well understood model that has been thoroughly described and studied. In our figures, lines corresponding to output from this model are given the label ‘Cole2000’.

- A model similar to the first, but with $\Omega_b = 0.04$, which is closer to current estimates. Since there are twice as many baryons as in the first model, if we leave the rest of the parameters unchanged then, as expected, the model is unable to match observations such as the luminosity function. Therefore we introduce a new physical process: thermal conduction in massive haloes (this is analysed in greater detail by Benson et al. 2003). We simply assume that gas is unable to cool if the halo circular velocity, V_{circ} , satisfies

$$V_{\text{circ}} > V_{\text{cond}} \sqrt{1+z} \quad , \quad (1)$$

where V_{cond} is a parameter we may adjust. This suppresses the problematic bright end of the luminosity function; the effect is similar, in fact, to more recent and more physically motivated implementations of feedback from active galactic nuclei in GALFORM (Bower et al. 2006). Though it is clearly rather crude, note that our

objective here is only to produce a realistic enough galaxy catalogue to compare to observations. We are trying to mimic the effect of whatever physical process suppresses the bright end of the luminosity function, without having to adopt a complicated parametrization that is no better physically motivated than a more simple and understandable one. The label we give to this model in our figures is ‘C2000hib’ (where ‘hib’ stands for ‘high baryon fraction’).

- Another model with $\Omega_b = 0.04$, but now incorporating ‘superwinds’. In this model it is postulated that a galaxy’s cold gas is heated strongly enough for it to be expelled completely from the halo, rather than returning to the reservoir of hot gas associated with the halo. In fact, the model is derived from that used by Baugh et al. (2005) to reproduce the abundance of faint galaxies detected at submillimetre wavelengths. This also incorporates the additions and refinements to GALFORM described by Benson et al. (2003). These include a modification to the assumed profile of the halo gas, a more sophisticated treatment of conduction, and a more detailed treatment of galaxy mergers, in particular the effects of tidal stripping and dynamical friction (Benson et al. 2002). They also include a simple model of the effect of reionization on small haloes, where cooling is prevented if $V_{\text{circ}} < V_{\text{cut}}$ and $z < z_{\text{cut}}$ for two parameters V_{cut} and z_{cut} . The strength of superwind feedback is parametrized by V_{SW} , the characteristic velocity of the wind. The model is denoted ‘Model M’ in our figures.

We wish to run each of these models in many different cosmologies, in order to generate galaxy catalogues in which the N -body component and the semi-analytic component are consistent. Changing cosmology naturally changes the galaxy population predicted by each model, however, so that even if we fix the parameters such that the galaxies match observational constraints in one fiducial cosmology, they are unlikely to match in other cosmologies. We therefore tweak the parameters between different cosmologies to try to match the data. It is not possible to do this for the full range of even the primary constraints described by Cole et al. (2000). We restrict ourselves to a comparison with the $^{0.1}r$ -band SDSS luminosity function of Blanton et al. (2003) at $z = 0.1$. Even then, to make the problem tractable and to ensure our three models remain distinct, we restrict the parameters we allow ourselves to vary to:

- V_{SW} , for Model M only.
- V_{cond} , for the C2000hib model only.
- V_{cut} , one of the parameters controlling reionization. Though we experimented with changing this for all the models, all the ones below have either $V_{\text{cut}} = 0$ (Cole2000 and C2000hib) or $V_{\text{cut}} = 60$ (Model M). As well as being simpler, this also helps make Model M more distinct from the other two.
- V_{hot} and α_{hot} . These are closely linked but we vary them independently. They control the strength of standard (i.e. not superwind) supernova feedback in the following way. The rate of change of the mass of hot gas and of cool gas in a halo are linked with the instantaneous star formation rate, ψ , by:

$$\dot{M}_{\text{hot}} = -\dot{M}_{\text{cool}} + \beta\psi \quad (2)$$

(Cole et al. 2000, equation 4.7). β is related to the circular velocity of the galaxy disc, V_{disc} , by

$$\beta = (V_{\text{disc}}/V_{\text{hot}})^{-\alpha_{\text{hot}}} \quad (3)$$

(Cole et al. 2000, equation 4.15).

Some of the cosmologies below require quite extreme, perhaps unphysical, parameter values. In some cases, GALFORM is

reluctant to run, while in others the fit for some observations is compromised in an attempt to fit the $^{0.1}r$ -band luminosity function well. In addition to running each model with tweaked parameters in each cosmology, therefore, we also run each model in each cosmology using the same parameters as the central cosmology of Run 1, in which $(\Omega_M, \sigma_8) = (0.3, 0.8)$.

We are not able to produce a good fit to the luminosity function in a χ^2 sense, even allowing these parameters to vary. This may be a concern when comparing clustering statistics to observational data. Volume-limited galaxy samples, to which we wish to compare our results later, are chosen such that all the galaxies are brighter than some given absolute magnitude limit. If we choose a sample of semi-analytic galaxies with the same magnitude limit, then because our luminosity function is wrong we may not be choosing a sample that necessarily corresponds to the observational one, even within our model. Therefore we instead select semi-analytic galaxy samples with a magnitude such that the sample has the same space density as the corresponding observational sample. This means that when we adjust the parameters of the model to match the luminosity function, it is more important for our purposes to match its overall *shape* rather than its magnitude normalization.

The Υ parameter of Cole et al. (2000) is related to this sort of scaling of the luminosity function. It was introduced to account for brown dwarfs, which absorb some of the mass of gas assumed to be tied up in stars, but without producing light. It is defined by

$$\Upsilon = \frac{\text{mass in visible stars} + \text{mass in brown dwarfs}}{\text{mass in visible stars}} \quad (4)$$

(Cole et al. 2000, equation 5.2). Clearly, then, we must have $\Upsilon \geq 1$ given this physical explanation. The result of including this effect is to scale luminosities by a factor $1/\Upsilon$. For each GALFORM model we run, we compare the resulting $^{0.1}r$ -band luminosity function with the observational value from the SDSS (in fact, we compare only one point near the characteristic luminosity, L_*). We express the difference between the two in terms of the Υ parameter: the (reciprocal of the) amount by which we would have to scale the luminosity of the semi-analytic galaxies to match the data. Sometimes this requires $\Upsilon < 1$. Therefore, when we give a value of Υ below, it should be treated only as an indication of the amount by which we would have to scale luminosities so that when we select a galaxy sample by a number density threshold then it would have the same luminosity threshold as the observational sample. Note that we calculate Υ by reference to a specific point on the SDSS $^{0.1}r$ -band luminosity function. Its exact value would change if we normalized at a different point (since the model luminosity function is not the same shape as the observational one), or in a different band (since the colour of model galaxies may be incorrect).

Once we have given ourselves the freedom to scale the luminosity function in this way, then, the effect of varying the parameters we allow ourselves to change to try to match the shape of the luminosity function is as follows:

- Increasing V_{SW} , or decreasing V_{cond} , tends to steepen the bright-end slope, i.e. give fewer very bright galaxies. V_{SW} is only non-zero for Model M; V_{cond} is only finite for the C2000hib model.
- Increasing V_{cut} reduces the slope at the faint end, reducing the number of the faintest of the galaxies we study.
- Increasing V_{hot} tends to suppress the overall space density of galaxies. Because of the effect of the other parameters, it is most useful for adjusting the abundance of galaxies of around L_* , or a little fainter.
- Changes in α_{hot} can be viewed as modulating the effect of changing V_{hot} . Visually, for typical values of V_{hot} , increasing α_{hot}

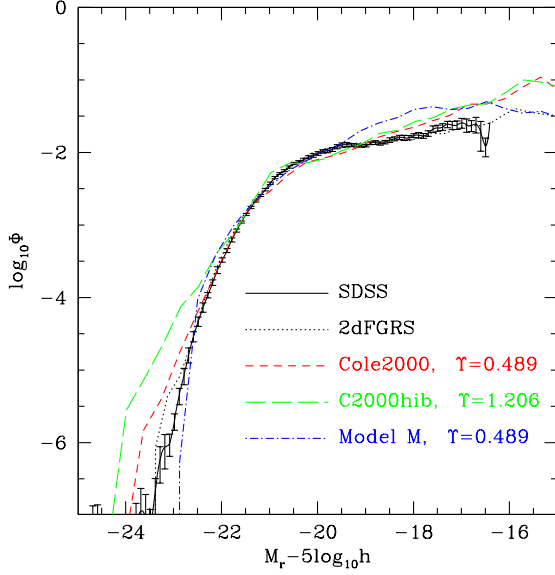


Figure 2. r -band luminosity functions for the three fiducial GALFORM models, compared to the SDSS luminosity function of Blanton et al. (2003) (solid line) and a 2dFGRS r -band luminosity function (dotted line, mostly obscured by the others) generated using the SuperCosmos r_F -band data (Hambly et al. 2001). The value of the scaling parameter Υ , required to normalize the model luminosities for galaxies of a particular space density in this band, is also given in the legend. Errors on the SDSS luminosity function are only given for every tenth point, for clarity.

flattens the faint-end slope, typically over a wider range of luminosities than V_{cut} .

We usually find that to make the bright-end slope steeper and to make the faint-end slope shallower, as required by the data, needs all parameters tweaked to give larger amounts of feedback. This tends to have the overall effect of reducing the predicted luminosities, leading to $\Upsilon < 1$ as mentioned above. Requiring $\Upsilon \geq 1$ would therefore require us to compromise one component or other of the shape in these models. Since we later rescale to match space densities anyway, we opt not to make this compromise. Given two parameter combinations which both match the luminosity function reasonably well and which both give $\Upsilon < 1$, we use the Υ parameter as a tie-breaker, selecting the combination which gives Υ closer to unity. We have also checked that each model is at least qualitatively consistent with the other primary GALFORM constraints (the Tully-Fisher relation, disc sizes, morphological mix, metallicities and gas fractions – see Cole et al. 2000).

The r -band luminosity function for each of our models in our fiducial cosmology ($\Omega_M = 0.3$ and $\sigma_8 = 0.8$) is shown in Fig. 2. Qualitatively, the agreement between the models and the data is reasonable. The very sharp cutoff at the bright end of the luminosity function in Model M is a generic feature of the model. The lower space density of very faint galaxies in this model is also generic, and comes from the introduction of reionization (non-zero V_{cut}). At first glance, it appears that the Cole2000 model gives better agreement with the data at the bright end than the C2000hib model, despite the inclusion of a feedback mechanism specifically to solve this problem in the latter. Recall, though, that the Cole2000 model has a lower baryon fraction, and despite this we have to introduce relatively high levels of supernova feedback to match the

shape of the luminosity function. We therefore need $\Upsilon \sim 0.5$ to recover the correct luminosities, while the C2000hib model needs a much more physically palatable $\Upsilon \sim 1.2$. It may appear that our requirement for $\Upsilon \sim 0.5$ is inconsistent with the original Cole et al. (2000) paper, the reference model of which requires $\Upsilon = 1.38$. It is not inconsistent, for a few reasons. Firstly, we use the label ‘Cole2000’ for our model because it uses equivalent code with the same physics governed by the same parameters as the models of Cole et al. (2000). As we have just noted, however, some of the parameters take different values in our fiducial model in order to try to match the shape of the r -band luminosity function. Secondly, while the reference model of Cole et al. (2000) had $\sigma_8 = 0.93$, ours has $\sigma_8 = 0.8$. Thirdly, their Υ was calculated by reference to the value of the observed b_J band luminosity function at L_* (though in fact the same correction also provided a good match to the K -band luminosity function). Ours is calculated by reference to the r -band luminosity function. We match to a point slightly brighter than L_* (where the exponential cutoff has started to bite more deeply and the galaxies are less abundant; the point at $M_r \sim -21.5$ can be seen quite easily in Fig. 2 as being where all the lines cross) since we otherwise had problems calculating Υ for some of our models with a very shallow faint-end slope and low galaxy number density.

2.3 Galaxy placement

With the N -body simulations and the semi-analytic catalogues in place, it remains to merge the two to create a synthetic galaxy catalogue, or in other words to populate the simulations with our galaxies. To each halo in the simulation we assign a semi-analytic galaxy population for a random merger tree of the same mass. We then place the central galaxy at the position of the particle with least gravitational potential energy, and place the satellite galaxies on random particles within the halo.

One might worry that given the resolution of our simulations, it is possible for the semi-analytic model to predict that a halo in a simulation contains a bright enough galaxy to enter our sample even though the halo is not resolved with at least 20 particles, which is our normal criterion for considering the halo to be resolved. To take account of these galaxies, we calculate the number of such haloes expected for the simulation volume for the Jenkins et al. (2001) mass function. We then take the galaxy populations predicted by GALFORM for these haloes and place the galaxies on random particles in the simulation which are not in haloes. We do not expect this to have a significant effect on clustering statistics, since almost all galaxies which would be placed in unresolved haloes are very faint, and in any case the halo bias as a function of mass is not strongly varying in this regime (Cole & Kaiser 1989; Mo et al. 1999) so that we do not lose too much accuracy by placing galaxies in haloes of the wrong mass. None the less, we have checked that employing this scheme has only a small effect on our measured correlation functions. Changing the minimum resolved mass from 20 particles to 50 particles has only a very small effect on the correlation function, as does ignoring the ‘unresolved’ galaxies entirely, even for a conservative mass limit of 50 particles. Moreover, this remains true even for galaxy samples which are rather faint when compared to the magnitude limit of the SDSS samples we will be considering, and which therefore provide a more stringent test.

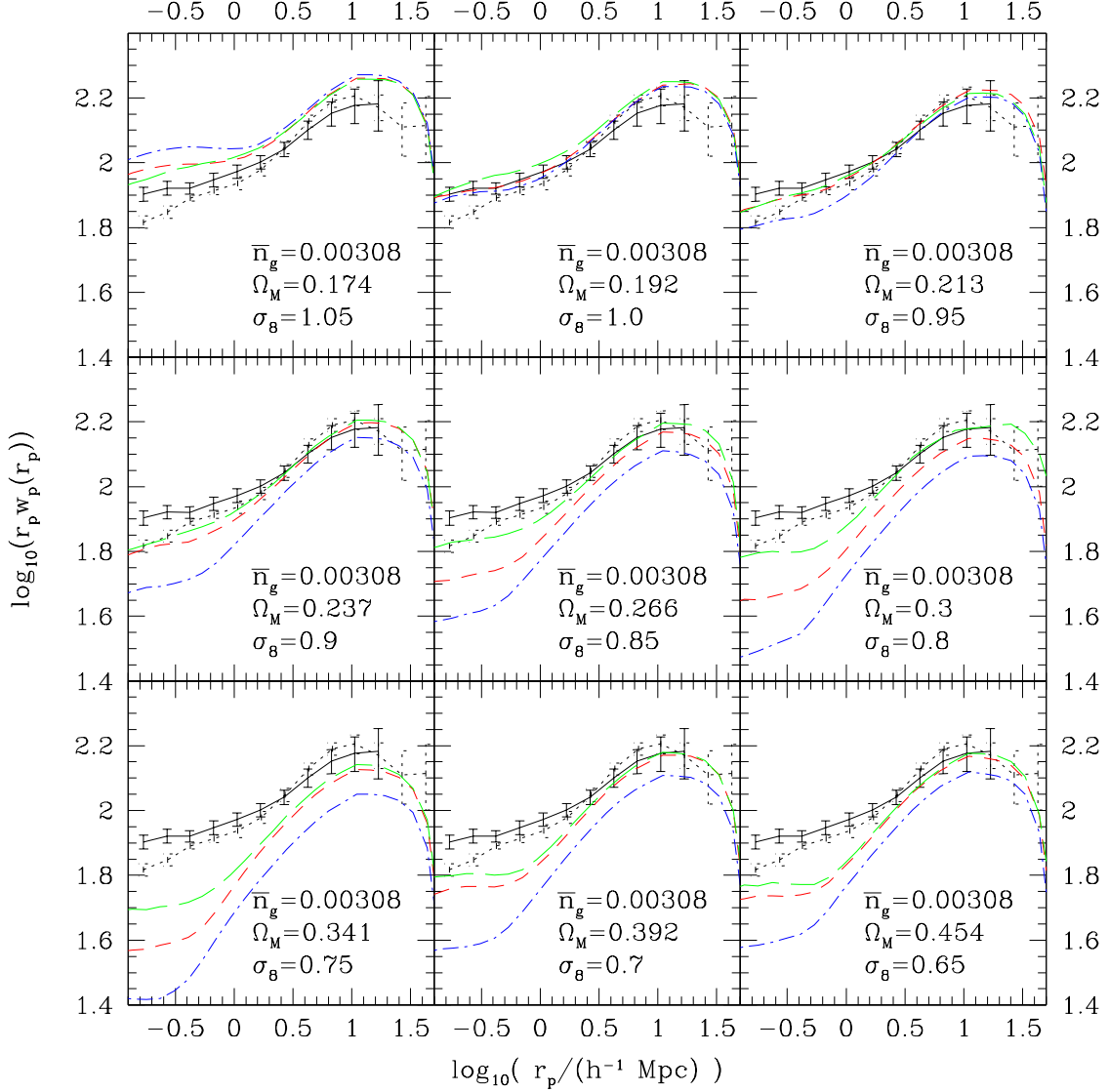


Figure 3. Clustering in our models and in the SDSS. $r_p w_p(r_p)$ is plotted for clarity. The solid, black line with error bars is the SDSS data; the dotted line shows the SDSS flux-limited sample for comparison. The coloured lines are from our three models: short-dashed red for Cole2000, long-dashed green for C2000hib and dot-dashed blue for Model M, as in Fig. 2. The nine different cosmologies form a grid in σ_8 with the cosmological parameters lying on the curve $\sigma_8 \Omega_M^{0.5} = 0.8(0.3)^{0.5}$. This plot shows models for which we allow ourselves to tweak the GALFORM parameters to match the luminosity function.

3 RESULTS

3.1 Observational samples

In their study of the luminosity and colour dependence of the galaxy correlation function using the main galaxy sample of the SDSS, Zehavi et al. (2005) calculated the projected two-point correlation function $w_p(r_p)$ for ten different galaxy samples defined by thresholds in absolute magnitude. We have been provided with these correlation functions, and their covariance matrices calculated by jackknife resampling. Zehavi et al. (2005) also tabulate the space density of each sample, so it is straightforward for us to select corresponding samples of semi-analytic galaxies.

Our cosmological constraints will use samples with a galaxy

space density $\bar{n}_g = 0.00308 h^3 \text{ Mpc}^{-3}$, corresponding to galaxies with $M_r - 5 \log_{10} h < -20.5$ in the SDSS. Our semi-analytic catalogues have approximately twice the effective volume of the observational sample, so when calculating how well our models fit the data we use only the covariance matrix of the observational correlation function to compute our errors, neglecting the statistical errors on the simulated function. We use the sample of this space density since it provides a good compromise between volume and space density, giving relatively small errors, and since most of the constraining power then comes from the galaxies of intermediate luminosity which are modelled best by the semi-analytic code. We will, though, briefly discuss the effect of using samples of a different space density or selected in a different waveband.

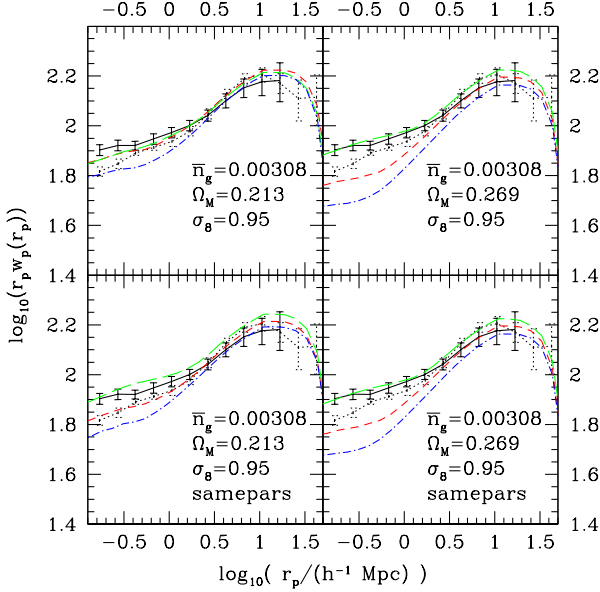


Figure 4. A comparison between our four sets of models for one particular value of σ_8 . The top two panels are for models in which we tweak the semi-analytic parameters to match the r -band luminosity function, while for the bottom two the parameters stay the same as for our fiducial model. The two left-hand panels are for the low- Ω_M cluster normalization curve while the others are for the high- Ω_M case. The colour coding and line styles of the models are the same as for Figs. 2 and 3.

3.2 Constraints

We compare the clustering in our synthetic catalogues and in the SDSS in Fig. 3. We plot the quantity $r_p w_p(r_p)$ since this scales out much of the r_p dependence and makes differences in shape easier to see. Fig. 3 shows our results for a grid of nine cosmologies spaced regularly in σ_8 such that they lie on the curve $\sigma_8 \Omega_M^{0.5} = 0.8(0.3)^{0.5}$ (‘Grid 1’). For this plot we show the models for which we allow the semi-analytic parameters to vary so as to provide a good match for the r -band luminosity function. Note that we have three other similar sets of models: one which includes the same cosmologies but in which the semi-analytic parameters are identical in each cosmology, and two more in which the cosmologies lie on the same grid in σ_8 but which have lower Ω_M , such that $\sigma_8 \Omega_M^{0.5} = 0.9(0.3)^{0.5}$ (‘Grid 2’). In one low- Ω_M sequence the semi-analytic parameters are allowed to vary, and in the other they are not. A figure similar to Fig. 3 could be made for each of the latter three sets of catalogues, but since the features turn out to be qualitatively similar we do not show such plots here. We do, though, compare the four sets for one particular value of σ_8 in Fig. 4. For each grid of cosmologies and for each choice as to whether to allow the parameters to vary we have catalogues for each of our three models, and therefore in total we have twelve sets of catalogues each of which has nine members lying on a regular grid in σ_8 . The key to our numbering of these sets is given in Table 2.

Examining Fig. 3, it is clear that some of our catalogues fit the data better than others. For the higher σ_8 cosmologies, the shape of the models fits that of the data rather well. The trend between cosmologies is consistent between the three GALFORM models: a higher amplitude of clustering for higher σ_8 , as expected. There are differences between the models, however, especially on small

Table 2. The key to the model numbering used in Fig. 5. The first column gives the label we assign to each of our 12 sets of populated simulations (each of which has nine cosmologies, regularly spaced in σ_8). The ‘Grid’ in the second column refers to whether the cosmologies lie on the cluster normalized curve with high Ω_M (Grid 1) or low Ω_M (Grid 2). The third column shows whether we adopt different parameters in different cosmologies, or whether they stay the same, while the fourth gives the GALFORM model in use.

Model no.	Grid	Same/diff. pars.	GALFORM model
1	1	diff.	C2000hib
2	1	diff.	Cole2000
3	1	diff.	M
4	1	same	C2000hib
5	1	same	Cole2000
6	1	same	M
7	2	diff.	C2000hib
8	2	diff.	Cole2000
9	2	diff.	M
10	2	same	C2000hib
11	2	same	Cole2000
12	2	same	M

scales, which must arise from differences in the details of the halo occupation distribution predicted by the models.

The variation in the predicted correlation function between cosmologies, and the consistent trend between models, supports our hope that comparison to the SDSS correlation function can constrain σ_8 . For each set of nine cosmologies, we calculate χ^2 with respect to the observed correlation function and its covariance matrix, then fit a quadratic through the three points around the minimum to interpolate and estimate the best-fitting σ_8 and its 1- σ error. The result of applying this procedure is given in Fig. 5. There, we give an estimate of σ_8 and its errors for each of our twelve different sets of populated simulations, as the black crosses and error bars. The model number referred to on the x -axis is explained in Table 2.

A few comments may be made about Fig. 5. Firstly, some of the sets of models yielded no value of σ_8 for which the simulated correlation function was an acceptable fit to the observed one. The large χ^2 and $\Delta\chi^2$ values then result in a spuriously small error bar. This is the case for models 9, 11 and 12, so the constraints coming from those models should be ignored. Secondly, recall that we ran only two N -body simulations, using only the outputs given in Table 1. In fact, while one was run with a larger value for σ_8 (and therefore a smaller Ω_M for an output with given σ_8), it was started with initial conditions where the different Fourier modes of the density field were given the same phase as in the low- σ_8 simulation. This means that the constraints from the different sets of synthetic galaxy catalogues are not independent, but should be used to give an indication of the systematic error arising from the choice of semi-analytic model parameters and the assumed value of Ω_M (which we do not constrain). Note that we have also plotted two constraints for each model in Fig. 5. On the left, with solid error bars, are the constraints derived just as we have described. We discuss the estimates on the right, with dashed error bars, in Section 3.3.1.

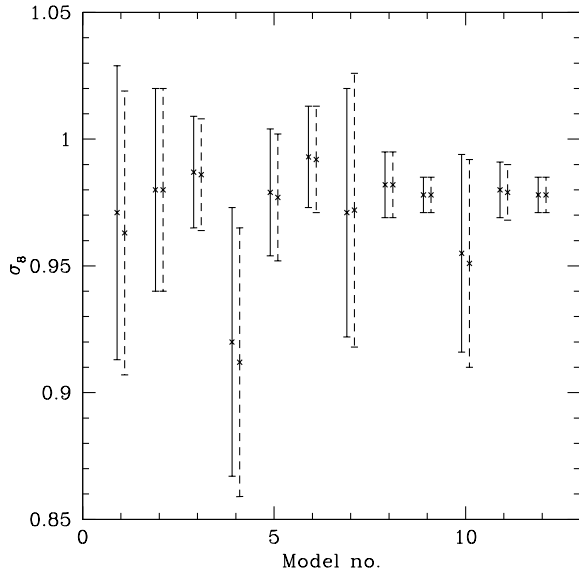


Figure 5. Constraints on σ_8 . The x -axis shows the model number, the key to which is given in Table 2. The y -axis shows the 1σ constraint on σ_8 achieved in that particular model. The points with solid error bars are for the unmodified catalogues. The points with dashed error bars show how the constraints change when we make an empirical correction for the effect of halo assembly bias (Croton, Gao & White 2007, and references therein). We do this by modifying the correlation function according to the scale-dependent bias between shuffled and unshuffled GALFORM catalogues in the Millennium Simulation, as described in Section 3.3.1.

3.3 Other catalogues

3.3.1 Halo assembly bias

The points with dashed error bars in Fig. 5 show a constraint after we attempt to correct our simulated correlation functions for the effect of so-called ‘halo assembly bias’. This is an effect that may arise if one of the assumptions we make when populating our simulation with galaxies is incorrect. We assume that the distribution from which the properties of the galaxy content of a halo are drawn depends only on the mass of the halo. In other words, since the halo merger tree is the basic input to our semi-analytic model, we assume that the distribution from which the properties of a halo’s merger tree are drawn depends only on halo mass. This is explicitly the case for the Monte Carlo merger trees we use here, since it is a result of the underlying extended Press-Schechter theory (Press & Schechter 1974; Bower 1991; Bond et al. 1991; Lacey & Cole 1993). This result was also supported by work on simulations (Lemson & Kauffmann 1999). More recently, however, the advent of larger simulations with better resolution has allowed this result to be challenged. Gao, Springel & White (2005) showed that old haloes of a given mass in the Millennium Simulation were more strongly clustered than young haloes of the same mass, while Harker et al. (2006) demonstrated that halo formation time is a function of halo environment as well as halo mass using an independent set of merger trees in the same simulation. Because halo age is a property of the halo merger tree, this shows that the assumption we have described is violated. In fact, the variation of N -body merger trees with environment has been studied in other large simulations (Maulbetsch et al. 2007). More generally, this environmental dependence formally invali-

dates the straightforward application of halo models of galaxy clustering (Benson et al. 2000; Seljak 2000; Berlind & Weinberg 2002; Cooray & Sheth 2002). It has stimulated theoretical attempts to explain the departure from the extended Press-Schechter prediction (e.g., Sandvik et al. 2007; Wang, Mo & Jing 2007), and to look for possible effects on the galaxy population both observationally (Yang, Mo & van den Bosch 2006) and in models (Croton et al. 2007; Zhu et al. 2006).

Our correlation functions are corrected using a GALFORM catalogue generated in the Millennium Simulation. The version of GALFORM which generates the catalogue takes as its input the actual N -body merger tree of each halo (Bower et al. 2006). This catalogue therefore incorporates environmentally dependent halo formation. In a similar spirit to Croton et al. (2007), we shuffle this catalogue, assigning to each halo the galaxy population of a random halo of the same mass. This destroys any connection between the environment of a halo of given mass and its galaxy population. We calculate the galaxy correlation function for a range of different magnitude thresholds for both the original and shuffled catalogues. This gives us an estimate of the effect of halo assembly bias, for GALFORM galaxies at least: we note that while our results are qualitatively consistent with those of Croton et al. (2007), the two semi-analytic models do not respond identically. We have calculated the scale-dependent ratio between the correlation functions, and then used this ratio (for a sample of appropriate space density) to correct the correlation functions used for our constraints. This is intended only to give an estimate of the size of the systematic error on our constraints coming from halo assembly bias. As Fig. 5 shows, the error from this source is small in comparison to the statistical errors, for our model at least.

3.3.2 Luminosity dependence

We calculate the correlation length of the samples by fitting a power law to $\xi(r)$ for $2 < r/(h^{-1} \text{ Mpc}) < 20$; that is, we parametrize the correlation function as $\xi(r) = (r/r_0)^{-\gamma}$ where r_0 is the correlation length. We have done this for all our samples of all luminosities, so we are able to plot the correlation length as a function of sample space density (or, equivalently, as a function of sample luminosity threshold) in Fig. 6. The black line in the plots shows the corresponding result from the SDSS. The SDSS data show a steady increase in clustering strength with luminosity (i.e. with decreasing space density) apart from a feature at $\bar{n}_g \approx 0.006 h^3 \text{ Mpc}^{-3}$ corresponding to the difference between two $M_r^{\text{max}} = -20.0$ samples: one has a large, overdense region at $z \sim 0.08$ excised (see Zehavi et al. 2005 for details) and has lower space density but, as might be expected, weaker clustering than the sample where this region is retained.

For many cosmologies, the Cole2000 model and the updated, higher baryon fraction C2000hib model do a reasonable job of matching the luminosity-dependent clustering in the SDSS, especially for samples of moderate to low space density. Model M, which invokes superwinds (see Section 2.2), does not do so well, predicting very little luminosity dependence. This may be because the feedback effects are so extreme in large haloes that their central galaxies are little brighter (if at all) than those at the centre of less massive, less biased haloes. The other two models tend to have the opposite problem in the brightest samples: they tend to predict too high an amplitude of clustering. This could be due to too tight a relationship between halo mass and galaxy luminosity (perhaps because in reality feedback is more efficient or more stochastic): none of the brightest galaxies is scattered into lower mass, less bi-

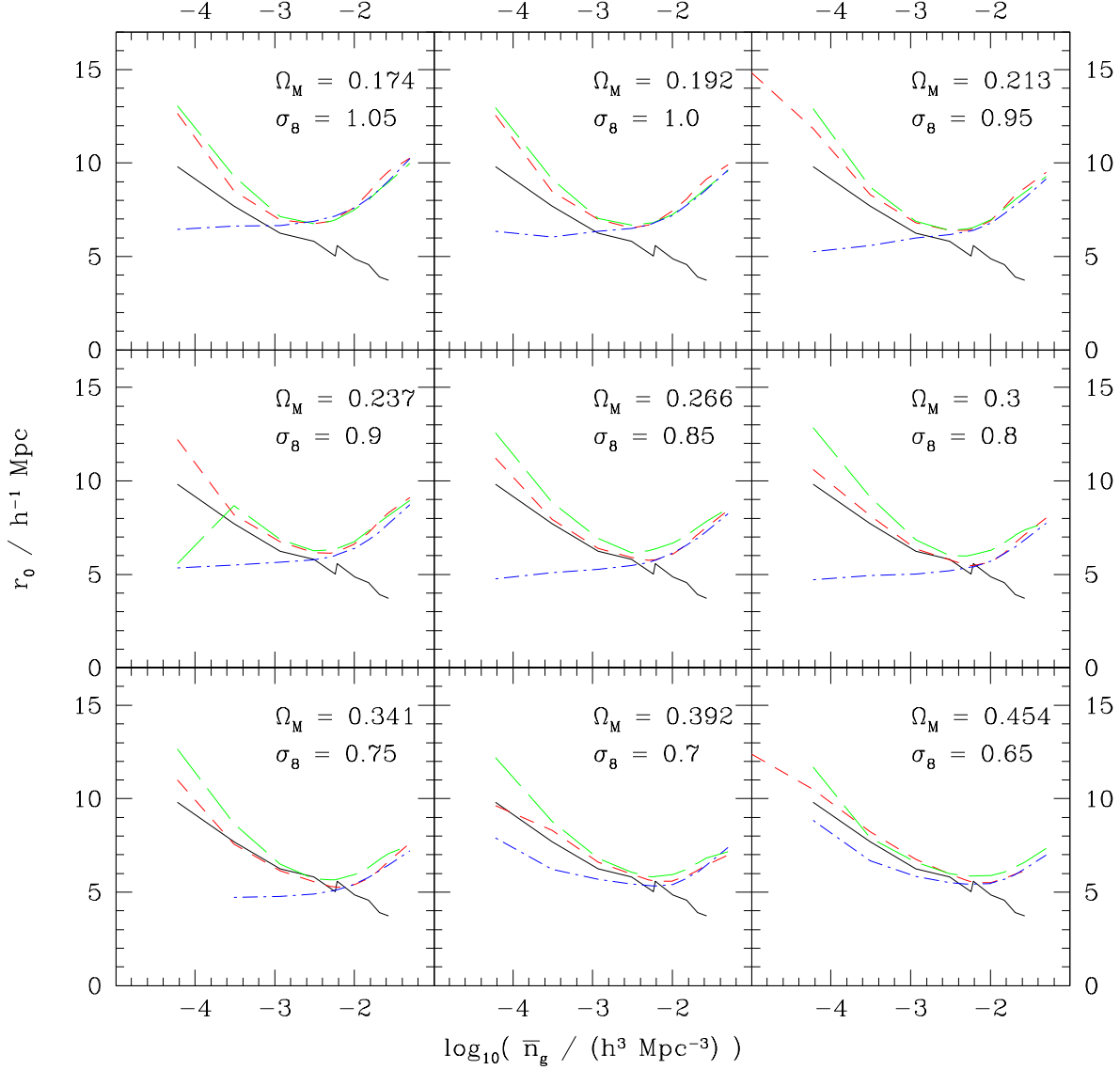


Figure 6. Correlation length as a function of sample space density for r -band selected galaxies, for the same set of models and with the same colour coding and line styles as Fig. 3.

ased haloes. A generic feature of the GALFORM models seems to be an upturn in the clustering amplitude at high space density. This suggests that too many of the faint galaxies generated by the model reside in high mass haloes. This may be related to the fact that it is hard to produce a luminosity function with a flat enough faint-end slope, the excess of faint galaxies perhaps consisting of satellites in massive haloes.

Clearly, matching the luminosity-dependent clustering of galaxies will continue to be a very stringent test for semi-analytic models. Even if the models were provided with the correct cosmology as an input, matching the clustering would still seem to require that the models predict the correct galaxy population for haloes as a function of luminosity and mass, rather than predicting quantities which implicitly average over a range of halo mass, such as the (unconditional) galaxy luminosity function. Conversely, if

the models were able to correctly capture the trends of luminosity dependent clustering, it would give us more confidence that they were predicting realistic galaxy populations on a halo-by-halo basis, and give a firmer foundation for attempts to constrain cosmology with methods involving semi-analytic catalogues. Though we bear this in mind, it seems unrealistic to require a perfect and complete model of galaxy formation before considering the information it can provide us on cosmological parameters.

The models display a minimum in clustering strength at roughly the space density of the sample we use for our constraint. We might therefore expect that using a sample of different space density may yield a lower estimate for σ_8 than the sample we have used above. In fact when we attempt to constrain σ_8 using different samples, we obtain high values of χ^2 for all cosmologies, even for those which appear by eye to be acceptable fits,

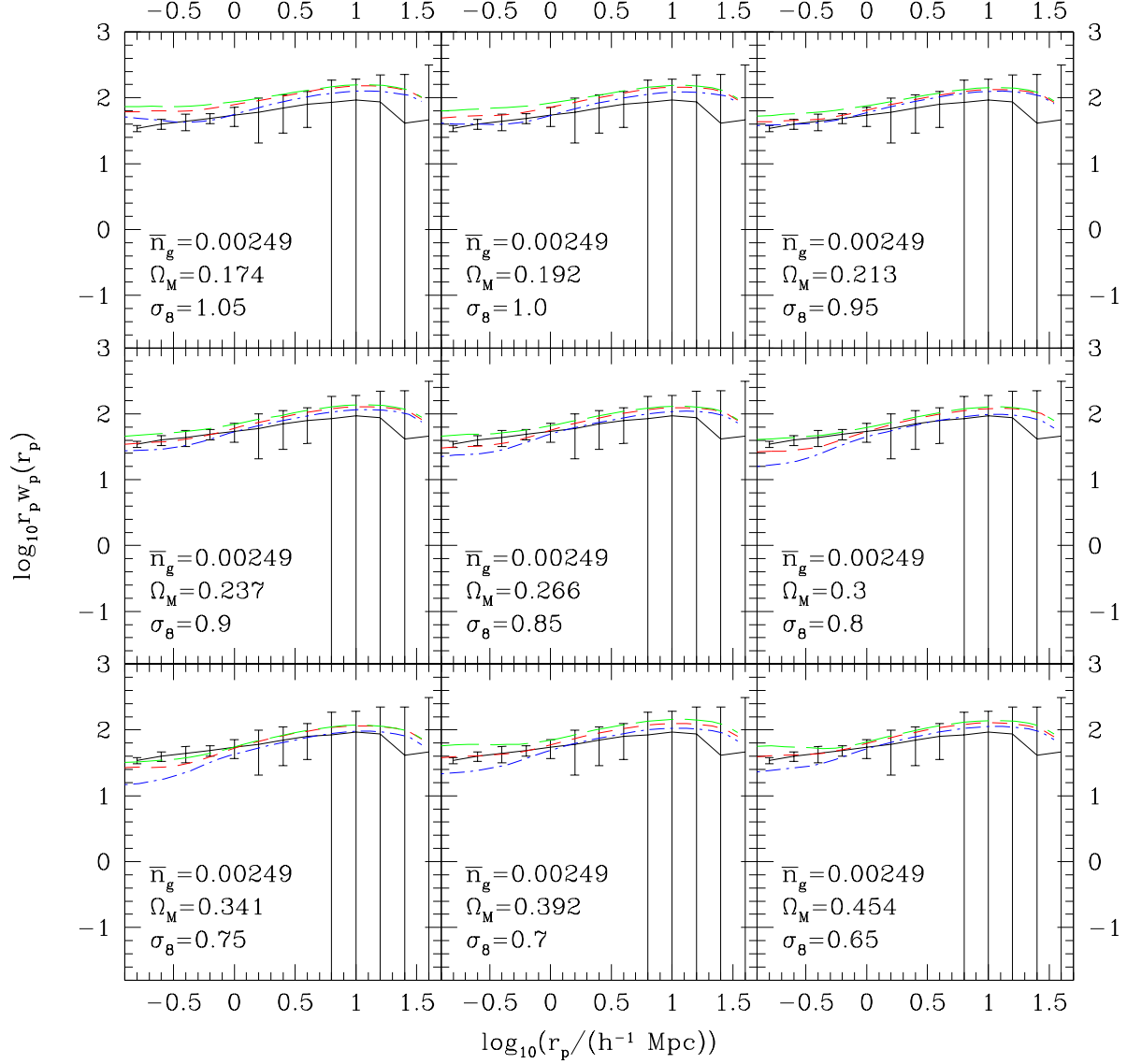


Figure 7. A plot similar to Fig. 3 but for a 2dF sample with $M_{b_J} - 5 \log_{10} h < -18$ and a b_J -selected GALFORM sample with space density $0.00249 \, h^3 \, \text{Mpc}^{-3}$.

or which give reasonable values of χ^2 using only the diagonal elements of the covariance matrix. We therefore suspect that for these samples, an estimate of σ_8 would be severely affected by noise in the covariance matrix. Using only the diagonal elements for samples with $\bar{n}_g = 0.00031$ or $0.01015 \, h^3 \, \text{Mpc}^{-3}$ (having $M_r - 5 \log_{10} h < -21.5$ and -19.5 respectively) would suggest a slightly lower σ_8 , in the region 0.85–0.9.

One might worry that the supercluster at $z \sim 0.08$ (mentioned above) affects our constraints. Zehavi et al. (2005) note, however, that in their analysis it has no effect on samples fainter than their $M_r - 5 \log_{10} h < -20.0$ sample, while removing it has a very small effect on brighter samples, producing a negligible drop in $w_p(r_p)$. If the drop were larger, then using samples without this region removed could bias our estimate of σ_8 upwards. More likely, the supercluster may cause a slight underestimate of the size of our

error bars, since the jackknife samples used to calculate the covariance matrix are smaller than the supercluster. This prevents the jackknife method from fully capturing the variance in the density field.

3.3.3 Constraints from the 2dFGRS

We have chosen to use the (r -band selected) SDSS rather than the (b_J -band selected) 2dFGRS for our main constraint on σ_8 , since the prediction for the luminosity of galaxies in bluer bands depends more heavily on recent star formation. It therefore tends to be more model-dependent than the prediction for redder bands, where there is a larger dependence on total stellar mass. None the less, the 2dFGRS provides very valuable data on galaxy clustering, and an accurate galaxy formation model should give constraints on σ_8 which

are consistent between the two datasets. In addition, the analysis of satellite fractions in the 2dFGRS by van den Bosch et al. (2005) suggested, if somewhat indirectly, that the 2dF data prefer a relatively low σ_8 . In a similar spirit to the analysis we perform here, this constraint on σ_8 came about independently of other datasets. It may therefore be interesting to see whether our relatively high value of σ_8 coming from galaxy clustering data alone is driven by the data (in which case our estimate for σ_8 when using 2dFGRS data should be consistent with theirs) or by other factors. Note, for example, that Pan & Szapudi (2005) quote a high preferred value for σ_8 in their 2dFGRS clustering analysis – albeit concentrating on the three-point function – though their error bar extends to low values, $\sigma_8 = 0.93^{+0.06}_{-0.2}$.

The 2dFGRS clustering data we use are an updated version of the analysis of Norberg et al. (2001, 2002) (Norberg et al., in prep.). This is the same dataset as used by Tinker et al. (2007) in their study of the luminosity dependence of the galaxy pairwise velocity dispersion. We compare the sample with $M_{b_J} - 5 \log_{10} h < -18$ to corresponding catalogues from our models in Fig. 7. The grid of models used is the same as for Fig. 3, but we select samples using a b_J magnitude threshold so as to match the space density of the 2dF sample. The threshold is chosen so that the space density, $0.00249 h^3 \text{ Mpc}^{-3}$, is similar to that of our main SDSS sample. The model clustering appears to depend more weakly on cosmology than for the r -selected samples, but there is still a clear trend and so we would hope still to be able to use these data to estimate σ_8 .

We calculate χ^2 between the data and the model using a principal component analysis, again ignoring the errors on the model correlation functions as we did for the SDSS. This analysis is performed on the dimensionless projected correlation function, $w_p(r_p)/r_p$, denoted $\Xi(\sigma)/\sigma$ by Norberg et al. (2002). We use only the first six principal components, which account for over 99 per cent of the variance. Statistical errors in the estimate of the principal components dominate the contribution to χ^2 of the less significant components. This illustrates the problems which would arise if we instead used the whole covariance matrix, as highlighted in Section 3.3.2.

The resulting constraints on σ_8 are given in Fig. 8. The model numbering is the same as for Fig. 5, and is given in Table 2. Noting the change in axis scale from Fig. 5, we see that the statistical error on σ_8 from the 2dF sample is comparable to that from the SDSS. While most of the grids of models yield σ_8 estimates similar to those obtained from the SDSS (if perhaps a little lower), there are several model grids which give significantly lower values of σ_8 for the b_J -selected samples than they did for the r -selected ones. In fact, these grids (numbers 1, 4 and 10) all use the C2000hib model. Our results therefore suggest that in this model the blue galaxies are more clustered than in the others, and hence lower dark matter clustering is required to match the observational result. This may be because the feedback excessively reddens isolated galaxies, leaving a larger proportion of the bluer galaxies in more massive, more clustered haloes. In any case it supports the idea that the clustering of model galaxies selected in bluer wavebands may be more dependent on the semi-analytic prescription.

4 DISCUSSION

As we note in Section 3.2, the constraints from the 12 different sets of catalogues in Fig. 5 are not independent, since the underlying N -body simulations in each case were seeded with the same phases.

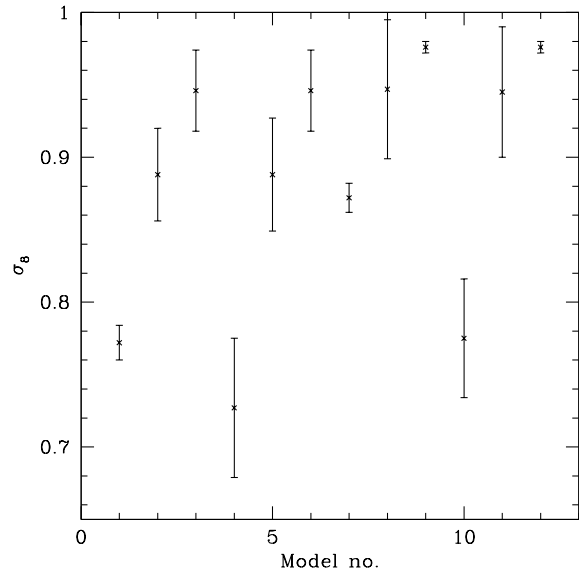


Figure 8. Constraints on σ_8 for the 2dF sample. The model numbering is the same as for Fig. 5 and is given in Table 2.

This does, though, mean that we can use the scatter between the catalogues to estimate the systematic error in the constraint arising from our choice of semi-analytic prescription. While we only have three different models (along with variants in which we do not tweak the parameters to match the r -band luminosity function), we can see that they differ quite strongly in the luminosity dependence (Fig. 3) and colour dependence (Fig. 8) of their clustering. They may, then, be representative of the scatter we can expect between GALFORM models that fit the r -band luminosity function and the primary constraints listed in Section 2.2. From the range of ~ 0.07 in the value of the best-fitting σ_8 between sets of catalogues, we estimate a systematic error from this source of ± 0.04 . The average size of the statistical error bars among the catalogues for which the best-fitting σ_8 was a good fit in a χ^2 sense suggests a statistical error of, again ± 0.04 . Adding these in errors in quadrature to the mean of the best-fitting values in these catalogues gives a final figure of $\sigma_8 = 0.97 \pm 0.06$ for the r -band samples.

Within the scope of the parameter variations we investigated, if we assume that $\sigma_8 = 0.8$ then none of our models gives us a good fit to the SDSS clustering over the full range of scales. This does not preclude the possibility that models that do not fit the luminosity function, or that include different physics to our particular semi-analytic model, may achieve such a fit.

Our value for σ_8 is clearly at odds with the most striking recent measurement, from the three-year WMAP data. Using those data alone, Spergel et al. (2007) quote $\sigma_8 = 0.761^{+0.049}_{-0.048}$ for flat, power-law Λ CDM, and this value is not significantly increased (though the error bars tighten) when the data are analysed jointly with galaxy clustering or supernova data. There is, though, some tension between the WMAP result and results from weak lensing surveys, which provide rather complementary parameter constraints (Tereno et al. 2005). Spergel et al.'s joint analysis of WMAP and the CFHTLS lensing survey (Hoekstra et al. 2006; Semboloni et al. 2006) pulls their estimate up to $\sigma_8 = 0.827^{+0.026}_{-0.025}$, with the lensing data alone favouring even higher values. Benjamin et al. (2007) have combined data from the CFHTLS

and other surveys to give $\sigma_8(\Omega_M/0.24)^{0.59} = 0.84 \pm 0.07$. Lyman- α forest data can be used to constrain the power spectrum; Seljak, Makarov, McDonald et al. (2005) quote $\sigma_8 = 0.90 \pm 0.03$ (reducing to 0.84 incorporating the new constraints on reionization from the three-year WMAP data). Measurements of cluster abundance have frequently been used to constrain σ_8 , but provide a very wide range of estimates because of the difficulty in relating the properties of an observed cluster to its mass (e.g., Rasia et al. 2005). Recent estimates are, though, consistent with the WMAP determination of σ_8 (e.g., Pierpaoli et al. 2003).

The overall picture of the value of σ_8 from other methods is therefore a little confusing, but even the highest recent estimates are only marginally consistent with ours. A possible source of tension between our constraints and those from WMAP is that we have assumed a spectral index $n_s = 1$, while the best-fitting WMAP σ_8 is quoted for their best-fitting n_s of approximately 0.95. As one can see from the lower right panel of figure 10 of Spergel et al. (2007), the constraints on these two parameters are correlated. Even so, increasing n_s to unity would only correspond to an increase in σ_8 of 0.1, which is not enough to eliminate the discrepancy with our result. A further complication is that the size of n_s is not the only difference in the initial $P(k)$ between the WMAP three-year constraints and our model. Though ideally one might like to repeat our tests using the power spectrum shape inferred by Spergel et al. (2007), we note that despite some parameter changes from the first-year WMAP constraints, the net change in the power spectrum is small. Furthermore, other datasets that are less dependent on n_s also prefer a lower σ_8 than we do, so even were we to infer a higher σ_8 from the CMB than currently favoured, our problems would not be solved.

As far as using galaxy data alone goes, methods involving higher-order correlations, particularly the three-point correlation function (or its Fourier counterpart the bispectrum) are promising, for example because of their ability to constrain galaxy bias. The addition of dynamical information, for example redshift space distortions or the pairwise velocity dispersion (PVD) can also help constrain cosmological parameters and galaxy bias. An analysis including PVD information in the conditional luminosity function (CLF) approach, by Yang et al. (2004, 2005), suggested relatively low values of σ_8 , though this was inferred from their models with high σ_8 since low- σ_8 simulations were not explicitly analysed. Results from halo occupation (HOD) modelling, an approach perhaps more akin to ours – for example the analysis of the cluster mass-to-light ratio by Tinker et al. (2005) – have tended also to favour a low σ_8 . Zheng & Weinberg (2007), and references therein, provide a detailed explanation of HOD modelling and its use in constraining parameters using galaxy data alone.

An alternative approach using the 2dFGRS is employed by van den Bosch et al. (2005). They study the abundance and radial distribution of satellite galaxies within the CLF framework, using mock galaxy catalogues produced by a semi-analytic code to calibrate their model. This calibration quantifies the impact of the inevitable imperfections in the halo finder that lead to satellite galaxies being spuriously identified as central galaxies of separate haloes, and vice versa. It also accounts for incompleteness effects in the 2dFGRS. Their results are consistent with other CLF analyses in suggesting that simultaneously matching the observed cluster mass-to-light ratio and the fraction of satellite galaxies in the 2dFGRS requires a low value of σ_8 , lowering the abundance of very massive haloes with a great number of satellites. Again, they do not directly construct mock galaxy redshift surveys for a low σ_8 model, but using the same calibration parameters as for their $\sigma_8 = 0.9$

model leads them to believe that adopting $\sigma_8 = 0.7$ provides a better fit to the data.

The parameters of the conditional luminosity functions which van den Bosch et al. (2005) use to fit the 2dFGRS data for low and high σ_8 are tabulated in their paper. We have used these parameters to construct the corresponding mean occupation functions – that is, the mean number of galaxies in a halo of given mass – then used these functions to populate the Millennium Simulation, and outputs of our Run 1 having $\sigma_8 = 0.7$ and $\sigma_8 = 0.9$. This is done as follows: for each halo in the simulation, we look up the mean number of galaxies in a halo of this mass, $\langle N(M) \rangle$. If $\langle N \rangle \leq 1$ the halo receives either a single, central galaxy (with probability $\langle N \rangle$) or no galaxies at all (with probability $1 - \langle N \rangle$). If $\langle N \rangle > 1$ then the halo receives a central galaxy, plus a number of satellite galaxies drawn from a Poisson distribution with mean $\langle N \rangle - 1$. The use of these probability distributions follows the work of Kravtsov et al. (2004) and Zheng et al. (2005); in addition, the halo occupation distribution of GALFORM galaxies in our models is consistent with this scheme. Once we know the number of galaxies in a given halo, we then place the galaxies according to the scheme described in Section 2.3.

We find that the mean occupation functions look reasonable, though in some cases they are not quite monotonic, and do not generally exhibit so clean a ‘step function + power law’ form as the GALFORM mean occupation functions. In our approach to populating simulations with the CLF HODs, we do not assign a luminosity to each galaxy, and so we construct a different catalogue for each magnitude threshold we wish to analyse. The space density of these catalogues as a function of magnitude gives us a cumulative luminosity function, and we have checked that this matches the 2dFGRS b_J -band luminosity function for the $\sigma_8 = 0.9$ catalogue, as it should by construction. For $\sigma_8 = 0.7$, the CLF catalogues give too steep a faint-end slope of the luminosity function, so that strictly speaking the CLF is incorrect, though this should not be a concern for galaxies of the luminosity we use for our clustering analysis. We also find that the CLF produces clustering consistent with our b_J -selected GALFORM samples.

The similar clustering in the GALFORM and CLF catalogues raises the question of what drives the difference in preferred σ_8 . The similarity between values from our SDSS and 2dF analyses suggests it is not driven entirely by the data. Moreover, it seems at odds with the conclusions of Tinker, Weinberg & Warren (2006), who show that in their HOD model the projected correlation function tightly constrains the satellite fraction. The answer may lie in the fact that their parametrized HOD, and our semi-analytic HOD, are unable to match the form of the mean occupation functions produced by the CLF approach, in which the parametrizations adopted for different parts of the CLF are a few steps removed from HOD parameters.

It would be exciting to conclude that our results support a real difference between low-redshift estimates of σ_8 (e.g. from weak lensing) and estimates using CMB data, and that this indicates something about, say, evolving dark energy. Other analyses find lower values, though, and there are still one or two concerns about our constraints. The mean occupation functions from our high Ω_M , low σ_8 GALFORM runs tend to be more ragged, perhaps indicating a difficulty with our modelling in these cosmologies. While we have checked that galaxy samples selected in a different waveband give similar results, the anomalous C2000hib model gives some cause for concern. Similarly, while samples with a different magnitude threshold appear to give consistent results, the luminosity dependence of clustering differs between models. These samples also

have smaller effective volume which seems to give rise to problems in the error analysis.

As we hoped, a large part of our constraint comes from the intermediate-scale clustering for which halo-based models are most necessary, but this is affected by the scheme for placing galaxies within haloes. The largest difference between our high and low σ_8 models (and between our low σ_8 models and the data) is manifested at small scales. The radial distribution of satellite galaxies within haloes is again different in the GALFORM model of Bower et al. (2006) which uses N -body substructure data, and this is clearly an area of galaxy formation modelling which requires further attention. We have repeated our analysis of the SDSS data using only points with $r_p > 2 h^{-1} \text{ Mpc}$. While the best-fitting value of σ_8 decreases by approximately six per cent to ~ 0.91 , the error bars approximately double in size, illustrating the importance of making use of smaller scales.

While bearing the above caveats in mind, we would like to emphasize the tight constraints available in principle using our technique, and to note that the results presented here are consistent (if marginally) with some other analyses which use only low-redshift data. If the tightness of the constraints seems surprising, consider firstly that in the absence of uncertainty about galaxy bias, the constraints would be extremely tight as the amplitude of the correlation function is very well determined. Secondly, by comparing model galaxies to real galaxies of the same abundance, we factor out most of the dependence on the details of the semi-analytic model. Any change that makes galaxies monotonically brighter or fainter will have no effect on our comparison between models and data. Thirdly, the number of galaxies assigned to each halo in the semi-analytic model is principally determined by the merger history of that halo, and this is well described by the extended Press-Schechter theory. Hence this is not a major uncertainty in the semi-analytic models: unlike purely statistical descriptions as provided by the HOD or CLF, our semi-analytic models do not have the freedom to define arbitrary HODs. These are instead largely determined by the merger trees.

We also remark that other constraints using galaxy data alone, which at first sight seem inconsistent with ours, use different techniques or different data or both. These inconsistencies arise even though galaxy formation models can reproduce statistics which implicitly average over a range of halo mass – such as the unconditional galaxy luminosity function – reasonably well. This illustrates that matching the luminosity- and colour-dependence of clustering, at small and large scales, is an important and very stringent requirement on galaxy formation models.

5 CONCLUSIONS

We have compared the SDSS projected two-point correlation function at a galaxy space density $\bar{n}_g = 0.00308 h^3 \text{ Mpc}^{-3}$ to a suite of populated simulations generated using the N -body code GADGET2 and the semi-analytic code GALFORM. Because we require N -body data in a great number of different cosmologies, we have relabelled and rescaled some simulation outputs using the techniques of Zheng et al. (2002) to avoid the need to run a full simulation for each cosmology in our grid. The galaxy catalogues are self-consistent, GALFORM being run afresh for each cosmology we study.

We have attempted to estimate the systematic error in our value of σ_8 due to the particular choice of semi-analytic model by running three different GALFORM variants in each cosmology. For

each of these variants we generate a catalogue in which the GALFORM parameters are adjusted to match the SDSS $^{0.1}r$ -band luminosity function and a catalogue in which the parameters take the same values as they take in the $(\Omega_M, \sigma_8) = (0.3, 0.8)$ cosmology. We obtain the result $\sigma_8 = 0.97 \pm 0.04(\text{statistical}) \pm 0.04(\text{systematic})$. This constraint is impressively tight, given we have attempted to narrow the range of assumptions we require to produce an estimate of σ_8 by using only one well understood, low redshift dataset. By choosing grids of cosmologies which lie on cluster-normalized curves, $\sigma_8 \Omega_M^{0.5} = \text{const.}$ we have shown that the degeneracies inherent in our approach are different to those inherent in cosmic shear measurements, which provide an important low redshift constraint on Ω_M and σ_8 . In fact our method gives an almost pure constraint on σ_8 . We have shown that in our model, halo assembly bias does not severely affect our constraint on σ_8 , though this may not be universally the case for other semi-analytic codes. If it were not the case, we would expect it to bias our estimate of σ_8 high, since failing to account for halo assembly bias tends to lower the amplitude of model correlation functions, requiring an increased σ_8 in the model to compensate.

We obtain similar values for σ_8 if we use samples with a lower or higher galaxy space density, but the error analysis is less secure. We also obtain similar values using a principal component analysis of 2dFGRS data, for a sample of similar space density to that used for our primary constraint. We note, though, that the clustering of galaxies selected in bluer wavebands appears to be more model-dependent, as one might expect.

Our estimate of σ_8 looks high compared to the values obtained by many recent measurements, in particular those from the WMAP experiment. While we note that this tension has some interesting consequences if it persists, we have also pointed out how apparent inconsistencies between our results and other low redshift constraints may arise. Small and intermediate scales in the correlation functions contribute strongly to χ^2 and hence to our constraint on σ_8 , and yet are not as well understood as the large scales. This is clearly an area where further modelling effort is required. Moreover, we will not be completely assured that semi-analytic models capture the phenomenology of the galaxy population sufficiently well for high precision cosmological constraints until they are able to match the observed colour- and luminosity-dependent clustering of galaxies. The models need to be able to reproduce the properties of the observed galaxy population on a halo-by-halo basis, not just the properties averaged spatially or over luminosity. This implies that if cosmological parameters can be tightly constrained by other techniques, measurements of galaxy clustering will continue to provide stringent tests for models of galaxy formation.

ACKNOWLEDGEMENTS

Most of the work for this paper was undertaken while GH was in receipt of a PhD studentship from the Particle Physics and Astronomy Research Council. Thanks to Peder Norberg for providing us with his principal component analysis of the 2dFGRS data, and his help with the use thereof. David Weinberg helped to initiate and plan this project, and provided the SDSS data on which our main analysis is based.

REFERENCES

Bardeen J. M., Bond J. R., Kaiser N., Szalay A. S., 1986, ApJ,

- 304, 15
- Bartelmann M., Doran M., Wetterich C., 2006, *A&A*, 454, 27
- Baugh C. M., Lacey C. G., Frenk C. S., Granato G. L., Silva L., Bressan A., Benson A. J., Cole S., 2005, *MNRAS*, 356, 1191
- Benjamin J., Heymans C., Semboloni E., Van Waerbeke L., Hoekstra H. et al., 2007, *MNRAS*, submitted (astro-ph/0703570)
- Benson A. J., Bower R. G., Frenk C. S., Lacey C. G., Baugh C. M., Cole S., 2003, *ApJ*, 599, 38
- Benson A. J., Cole S., Frenk C. S., Baugh C. M., Lacey C. G., 2000, *MNRAS*, 311, 793
- Benson A. J., Lacey C. G., Baugh C. M., Cole S., Frenk C. S., 2002, *MNRAS*, 333, 156
- Berlind A. A., Weinberg D. H., 2002, *ApJ*, 575, 587
- Blanton M. R. et al., 2003, *ApJ*, 592, 819
- Bond J. R., Cole S., Efstathiou G., Kaiser N., 1991, *ApJ*, 379, 440
- Bower R. G., 1991, *MNRAS*, 248, 332
- Bower R. G., Benson A. J., Malbon R., Helly J. C., Frenk C. S., Baugh C. M., Cole S., Lacey C. G., 2006, *MNRAS*, 370, 645
- Cole S., Helly J., Frenk C. S., Parkinson H., 2007, *MNRAS*, submitted (astro-ph/07081376)
- Cole S., Kaiser N., 1989, *MNRAS*, 237, 1127
- Cole S., Lacey C. G., Baugh C. M., Frenk C. S., 2000, *MNRAS*, 319, 168
- Cole S., Percival W. J., Peacock J. A., Norberg P., Baugh C. M., Frenk C. S. et al., 2005, *MNRAS*, 362, 505
- Coles P., 1993, *MNRAS*, 262, 1065
- Cooray A., Sheth R., 2002, *Physics Reports*, 372, 1
- Croton D. J., Gao L., White S. D. M., 2007, *MNRAS*, 374, 1303
- Croton D. J., Springel V., White S. D. M., De Lucia G. et al., 2006, *MNRAS*, 365, 11
- Davis M., Efstathiou G., Frenk C. S., White S. D. M., 1985, *ApJ*, 292, 371
- De Lucia G., Springel V., White S. D. M., Croton D., Kauffmann G., 2006, *MNRAS*, 366, 499
- Doran M., Schwindt J.-M., Wetterich C., 2001, *Phys. Rev. D*, 64, 123520
- Eisenstein D. J., Zehavi I., Hogg D. W., Scoccimarro R. et al., 2005, *ApJ*, 633, 560
- Eke V. R., Cole S., Frenk C. S., 1996, *MNRAS*, 282, 263
- Gao L., Springel V., White S. D. M., 2005, *MNRAS*, 363, L66
- Hambly N. C. et al., 2001, *MNRAS*, 326, 1279
- Harker G., Cole S., Helly J., Frenk C., Jenkins A., 2006, *MNRAS*, 367, 1039
- Hoekstra H. et al., 2006, *ApJ*, 647, 116
- Jenkins A., Frenk C. S., White S. D. M., Colberg J. M., Cole S., Evrard A. E., Couchman H. M. P., Yoshida N., 2001, *MNRAS*, 321, 372
- Kravtsov A. V., Berlind A. A., Wechsler R. H., Klypin A. A., Gottlöber S., Allgood B., Primack J. R., 2004, *ApJ*, 609, 35
- Lacey C., Cole S., 1993, *MNRAS*, 262, 627
- Lemson G., Kauffmann G., 1999, *MNRAS*, 302, 111
- Maulbetsch C., Avila-Reese V., Colín P., Gottlöber S., Khalatyan A., Steinmetz M., 2007, *ApJ*, 654, 53
- Mo H. J., Mao S., White S. D. M., 1999, *MNRAS*, 304, 175
- Neistein E., Dekel A., 2007, *MNRAS*, submitted (astro-ph/07081599)
- Norberg P., Baugh C. M., Hawkins E., Maddox S., Madgwick D., Lahav O., Cole S., Frenk C. S. et al., 2002, *MNRAS*, 332, 827
- Norberg P., Baugh C. M., Hawkins E., Maddox S., Peacock J. A., Cole S., Frenk C. S. et al., 2001, *MNRAS*, 328, 64
- O'Meara J. M., Tytler D., Kirkman D., Suzuki N., Prochaska J. X., Lubin D., Wolfe A. M., 2001, *ApJ*, 552, 718
- Pan J., Szapudi I., 2005, *MNRAS*, 362, 1363
- Parkinson H., Cole S., Helly J., 2007, *MNRAS*, submitted (astro-ph/07081382)
- Peacock J. A., 2003, astro-ph/0309240
- Pierpaoli E., Borgani S., Scott D., White M., 2003, *MNRAS*, 342, 163
- Press W. H., Schechter P., 1974, *ApJ*, 187, 425
- Rasia E., Mazzotta P., Borgani S., Moscardini L., Dolag K., Tormen G., Diaferio A., Murante G., 2005, *ApJL*, 618, L1
- Refregier A., 2003, *ARA&A*, 41, 645
- Sandvik H. B., Möller O., Lee J., White S. D. M., 2007, *MNRAS*, 377, 234
- Seljak U., 2000, *MNRAS*, 318, 203
- Seljak U., Makarov A., McDonald P. et al., 2005, *Phys. Rev. D*, 71, 103515
- Seljak U., Zaldarriaga M., 1996, *ApJ*, 469, 437
- Semboloni E. et al., 2006, *A&A*, 452, 51
- Smith R. E. et al., 2003, *MNRAS*, 341, 1311
- Spergel D. N., Bean R., Doré O., Nolte M. R. et al., 2007, *ApJS*, 170, 377
- Spergel D. N., Verde L., Peiris H. V., Komatsu E., Nolte M. R. et al., 2003, *ApJS*, 148, 175
- Springel V., 2005, *MNRAS*, 364, 1105
- Springel V. et al., 2005, *Nature*, 435, 629
- Springel V., White S. D. M., Tormen G., Kauffmann G., 2001, *MNRAS*, 328, 726
- Springel V., Yoshida N., White S. D. M., 2001, *New Astronomy*, 6, 79
- Tereno I., Doré O., van Waerbeke L., Mellier Y., 2005, *A&A*, 429, 383
- Tinker J. L., Norberg P., Weinberg D. H., Warren M. S., 2007, *ApJ*, 659, 877
- Tinker J. L., Weinberg D. H., Warren M. S., 2006, *ApJ*, 647, 737
- Tinker J. L., Weinberg D. H., Zheng Z., Zehavi I., 2005, *ApJ*, 631, 41
- van den Bosch F. C., Yang X., Mo H. J., Norberg P., 2005, *MNRAS*, 356, 1233
- Wang H. Y., Mo H. J., Jing Y. P., 2007, *MNRAS*, 375, 633
- Yang X., Mo H. J., Jing Y. P., van den Bosch F. C., Chu Y., 2004, *MNRAS*, 350, 1153
- Yang X., Mo H. J., van den Bosch F. C., 2006, *ApJL*, 638, L55
- Yang X., Mo H. J., van den Bosch F. C., Jing Y. P., 2005, *MNRAS*, 356, 1293
- Zehavi I. et al., 2005, *ApJ*, 630, 1
- Zheng Z., Berlind A. A., Weinberg D. H., Benson A. J. et al., 2005, *ApJ*, 633, 791
- Zheng Z., Tinker J. L., Weinberg D. H., Berlind A. A., 2002, *ApJ*, 575, 617
- Zheng Z., Weinberg D. H., 2007, *ApJ*, 659, 1
- Zhu G., Zheng Z., Lin W. P., Jing Y. P., Kang X., Gao L., 2006, *ApJL*, 639, L5